PAPER • OPEN ACCESS

Opinion competition dynamics on multiplex networks

View the article online for updates and enhancements.

New Journal of Physics

The open access journal at the forefront of physics

CrossMark

OPEN ACCESS

PAPER

Opinion competition dynamics on multiplex networks

R Amato[1,2] ⓘ, N E Kouvaris[3] ⓘ, M San Miguel[4] ⓘ and A Díaz-Guilera[1,2] ⓘ

[1] Departament de Física de la Matèria Condensada, Universitat de Barcelona, Martí i Franquès 1, E-08028 Barcelona, Spain
[2] Universitat de Barcelona Institute of Complex Systems (UBICS), Universitat de Barcelona, Barcelona, Spain
[3] naXys, Namur Institute for Complex Systems, University of Namur, rempart de la Vierge 8, B 5000 Namur, Belgium
[4] IFISC (CSIC-UIB), E-07122 Palma de Mallorca, Spain

E-mail: amato@ub.edu

Abstract

Multilayer and multiplex networks represent a good proxy for the description of social phenomena where social structure is important and can have different origins. Here, we propose a model of opinion competition where individuals are organized according to two different structures in two layers. Agents exchange opinions according to the Abrams–Strogatz model in each layer separately and opinions can be copied across layers by the same individual. In each layer a different opinion is dominant, so each layer has a different absorbing state. Consensus in one opinion is not the only possible stable solution because of the interaction between the two layers. A new mean field solution has been found where both opinions coexist. In a finite system there is a long transient time for the dynamical coexistence of both opinions. However, the system ends in a consensus state due to finite size effects. We analyze sparse topologies in the two layers and the existence of positive correlations between them, which enables the coexistence of inter-layer groups of agents sharing the same opinion.

1. Introduction

Human interaction often gives rise to different phenomena of collective agreement ranging from common language or religion to opinion formation. Various models have been proposed [1–4] to describe the process of social consensus, with the so-called *voter model* being one of the simplest and most studied [5]. It is a model with two equivalent states, first introduced to describe competition in biological species [5], and later named as the voter model in [6]. Voter dynamics is based on the mechanism of *imitation,* in which individuals change their opinion by imitating their randomly selected neighbors [1, 7, 8]. The model has two absorbing states of consensus (collective agreement in one of the states) and a critical dimension. In dimension $d = 1, 2$ there is coarsening with the unbounded growth of domains of each of the absorbing states. For $d > 2$, including typical complex networks, there is no coarsening and the system only reaches an absorbing state through finite size fluctuations. In the infinite system limit, the system remains in an active dynamical state with the two states coexisting [1, 7].

A population model which aimed to describe the competition of two languages was proposed by Abrams and Strogatz (AS) [9]. It turns out that the AS model is a mean-field approximation of an individual based model, which is a modification of the voter model [10]. The two options here are two non-equivalent languages which compete in a bilingual society. The languages are not perceived by the individuals in the same way, they have complementary *prestiges* reflecting the difference in the social status of spoken languages. An additional parameter, the *volatility*, was introduced in the latter model to indicate the tendency to switch the use of a language. The AS model fits the real aggregated data of endangered languages such as Quechua (in competition with Spanish), and Scottish Gaelic and Welsh (both in competition with English) [11, 12]. Moreover, as has been found by Vazquez *et al* [13], the AS model can support steady states where both languages coexist for small values of volatility. Several studies [1, 2, 13–15] have been inspired by the AS model, which tests how different formalization of the interactions—e.g. different network topology—can determine dominance by one state or, in contrast, when configurations in which two states coexist is possible.

In recent years, similar studies have been performed on more complex structures: the so-called *multiplex networks* [16, 17]. A multiplex network [18–22] consists of two or more interconnected networks lying in distinct layers. The layers have the same number of nodes, which are connected to their counterparts across the layers, and in general have a different connectivity structure within them [18, 20]. This framework allows for a more realistic approach in the study of the interaction of individuals, which can communicate through different types of channel. Multiplex networks have been used to analyze public transportation systems [23, 24], the spreading of awareness and infection [25, 26], the dynamics of ecological populations [27, 28], cultural dynamics [29] and the evolution of social networks [17, 30].

More recently, Diakonova *et al* [16] demonstrated the irreducibility of a multiplex version of the voter model. In this approach, a multiplex network was considered, where a fraction of nodes and links can be present in both layers and any change in the state of those nodes in a layer is instantly replicated by the other. This mechanism affects voter model dynamics, and significant differences from the classical single layer case were found.

Here we propose a modification of the voter model organized in a multiplex network, where the dynamics occurring on the nodes is irreducible by nature. Specifically, each node can appear in a different state and may receive concurrent social pressures in distinct layers. Additionally, the state of a node in one layer influences its own state in the other layer. This system paves the way for new scenarios for the coexistence of opposing options, which are discussed in this article. Starting from microscopic dynamics, we develop a mean field theory which shows that in addition to consensus, there is a non-trivial steady state (the non-consensus states), where the two options coexist simultaneously, emerge and are linearly stable. Our theoretical findings were verified by numerical simulations, where, however, no-consensus states can lose their stability due to finite size effects and the system is eventually driven to consensus. Nonetheless, the time needed for the individuals to consent is longer than in single-layer networks. We analyze this behavior by developing a probabilistic macroscopic description. We show that the coupling of two layers, fully connected, or Erdös–Rényi networks, with two different preferred options can generate various kinds of coexistence options. In addition, we analyze how the topology of the two networks and the correlations between layers can influence the distribution of states among nodes. Specifically, we observe that links overlap the correlation, together with degree-degree correlation between the layers, promoting the formation of inter-layer groups of nodes in the same state.

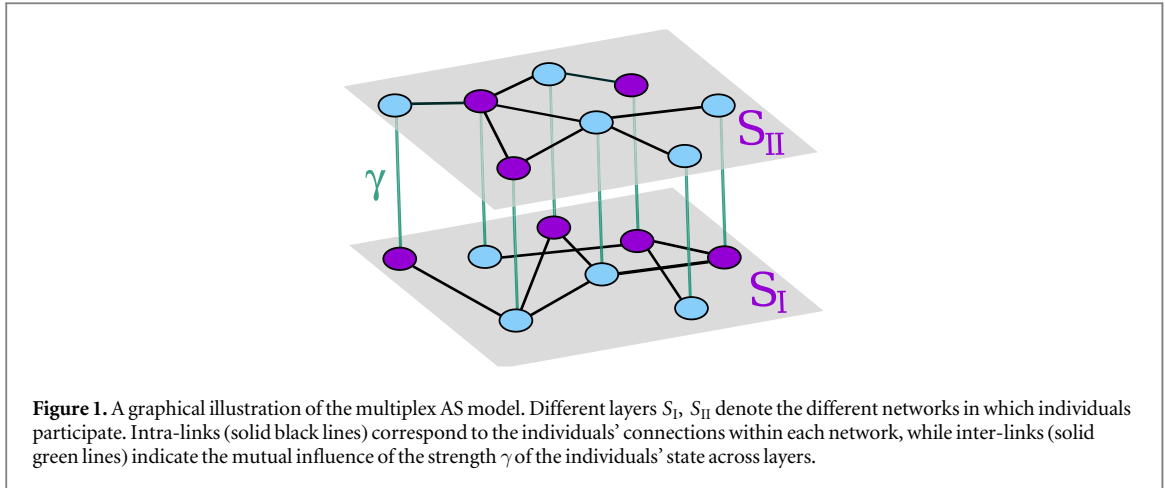## 2. Competition of options on multiplex networks

We propose here a model for describing the competition between two abstract options, A and B (they can be languages, opinions, voting intention, etc) in a multiplex network. The model is based on a modification of the AS model with volatility equal to one, and keeping the idea that the two options have different perceived status. In this model social interactions occur within distinct layers that may have originated from different contexts like family or business networks, Facebook or Twitter, etc. Nodes and their counterparts across layers correspond to the same individuals participating in different networks. Intra-layer links denote the individuals' connections within each network, while inter-layer links indicate the mutual influence of the individuals' state across layers (see figure 1).

We assign a state σ_i^α to each node i ($i = 1, 2, \dots N$) in the layer α ($\alpha = $ I, II), such that $\sigma_i^\alpha = 1$ (or 0) if the node is option A (or B) in layer α. We also endow prestige S_α to option A differently in each layer; the corresponding option B has a complementary prestige $1 - S_\alpha$. We restrict the values of the prestiges to $S_I \in [0.5, 1]$ and $S_{II} \in [0, 0.5]$, in order to guarantee that the two layers do not have the same preferred option. The state of a node in a layer influences its own state in the other layer with strength γ, where $0 \leqslant \gamma \leqslant 1$. The limited values of γ correspond to opposing situations so, $\gamma = 0$ denotes that the two layers are independent, while $\gamma = 1$ represents a situation in which individuals are not influenced by their neighbors.

The dynamical evolution of this multiplex-organized system is described below. A randomly chosen node i in one layer can change its option according to the transition probabilities,

$$P_{i,A \to B}^\alpha = (1 - \gamma)(1 - S_\alpha)\left(1 - \frac{1}{k_i^\alpha}\sum_{j=1}^N G_{ij}^\alpha \sigma_{ij}^\alpha\right) + \gamma(1 - \sigma_i^{\bar\alpha}),$$

$$P_{i,B \to A}^\alpha = (1 - \gamma)S_\alpha \frac{1}{k_i^\alpha}\sum_{j=1}^N G_{ij}^\alpha \sigma_{ij}^\alpha + \gamma\sigma_i^{\bar\alpha}, \qquad (1)$$

where G_{ij}^α is the adjacency matrix of layer α, with elements $G_{ij}^\alpha = 1$, if nodes i and j are connected in layer α and $G_{ij}^\alpha = 0$ otherwise, k_i^α is the degree of the node i in layer α, and with $\sigma_i^{\bar\alpha}$ we denote the state of the node i in the other layer.

Figure 1. A graphical illustration of the multiplex AS model. Different layers S_I, S_{II} denote the different networks in which individuals participate. Intra-links (solid black lines) correspond to the individuals' connections within each network, while inter-links (solid green lines) indicate the mutual influence of the strength γ of the individuals' state across layers.

System equation (1) supports steady states of full consensus where all individuals appear to have a single option A or B. However, the multiplex structure of this model induces a new steady state, which has never been observed in the classical voter model, where the two options coexist. In the following we present the stability analysis of these steady states starting with a mean field (MF) description of the dynamics. Then, we build a theory for the ordering dynamics to analyze the system's evolution towards a steady state. We also perform a numerical simulation on complete (all-to-all) and Erdös–Rényi networks in order to verify our theoretical findings.

3. Mean field approach and master equation

One of the central problems in the analysis of opinion dynamics is understanding the conditions in which a collective agreement occurs. The dynamical evolution of system equation (1) is analyzed by means of an MF approach, where a previously used order parameter for the single-layer networks [13, 31] is employed. The state of the system is characterized by the option's polarization (often called magnetization) and is defined as the difference between the fractions X_α of nodes in state 1 (option A) and the fractions $1 - X_\alpha$ of nodes in state 0 (option B). Therefore, for layer α we obtain the polarization option

$$m_\alpha = X_\alpha - (1 - X_\alpha) = 2X_\alpha - 1, \tag{2}$$

which defines the state of the system and lies in the interval $[-1, 1]$, where $m_\alpha = -1$ denotes the winning option B and $m_\alpha = 1$ of option A.

The dynamics of the system is governed by the presence of *active links*, namely of links connecting nodes in different states, because the probability of a node switching to another state depends on the density of its active links. Two types of active link are associated with each node: active intra-layer links if the node in layer α does not consent with its neighbors in α, and active inter-layer links if it has a different state in the different layers. The density of active intra-layer links in layer α is given by the expression,

$$\rho_\alpha = \frac{1}{2L^\alpha} \sum_{i=1}^{N} \sum_{j=1}^{N} G_{ij}^\alpha (1 - \delta_{\sigma_i^\alpha, \sigma_j^\alpha}), \tag{3}$$

where $\alpha = I$, II, δ is Kronecker's delta and L^α is the total number of links in layer α. The density of the active inter-layer links reads

$$\rho_\perp = \frac{1}{N} \sum_{i=1}^{N} (1 - \delta_{\sigma_i^I, \sigma_i^{II}}). \tag{4}$$

In the employed MF approximation, each node in a layer is connected with all the other nodes of that layer. Therefore, we can naturally express the densities of intra-layer and inter-layer active links as a function of m_α as,

$$\rho_\alpha = 2X_\alpha(1 - X_\alpha) = \frac{1}{2}(1 - m_\alpha^2) \tag{5}$$

and

$$\rho_\perp = X_I + X_{II} - 2X_I X_{II} = \frac{1}{2}(1 - m_I m_{II}). \tag{6}$$

In the appendix we derive the master equation for the probability $Q(m_\alpha, t)$ that the system has polarization option m_α at time t

$$\partial_t Q_\alpha = -\partial_{m_\alpha}[\partial_{m_\alpha} V Q_\alpha] + \frac{1}{2N}\partial_{m_\alpha}^2[D_\alpha Q_\alpha], \tag{7}$$

where

$$\begin{aligned} \partial_{m_\alpha} V &= (1-\gamma)(2S_\alpha - 1)\rho_\alpha + \gamma(m_{\bar\alpha} - m_\alpha), \\ D_\alpha &= (1-\gamma)\rho_\alpha + \gamma\rho_\perp. \end{aligned} \tag{8}$$

We notice that the influence of each layer on the other appears not only in the potential but also as an additive term in the diffusion coefficient. We can say that term $\rho_\perp$ controls the diffusion of the two options in the two layers. The two potentials felt by the two layers have an opposite minimum because of the setting in the prestiges; for $\gamma = 0$ each layer would reach the full consensus in opposite options.

In the thermodynamic limit the diffusive term is canceled and the potential $V(m_I, m_{II})$ defined in equation (8) has three extrema:

1. Two corresponding to the states of full consensus:

    (a) $(m_I, m_{II}) = (1, 1)$ (consensus to A)

    (b) $(m_I, m_{II}) = (-1, -1)$ (consensus to B)

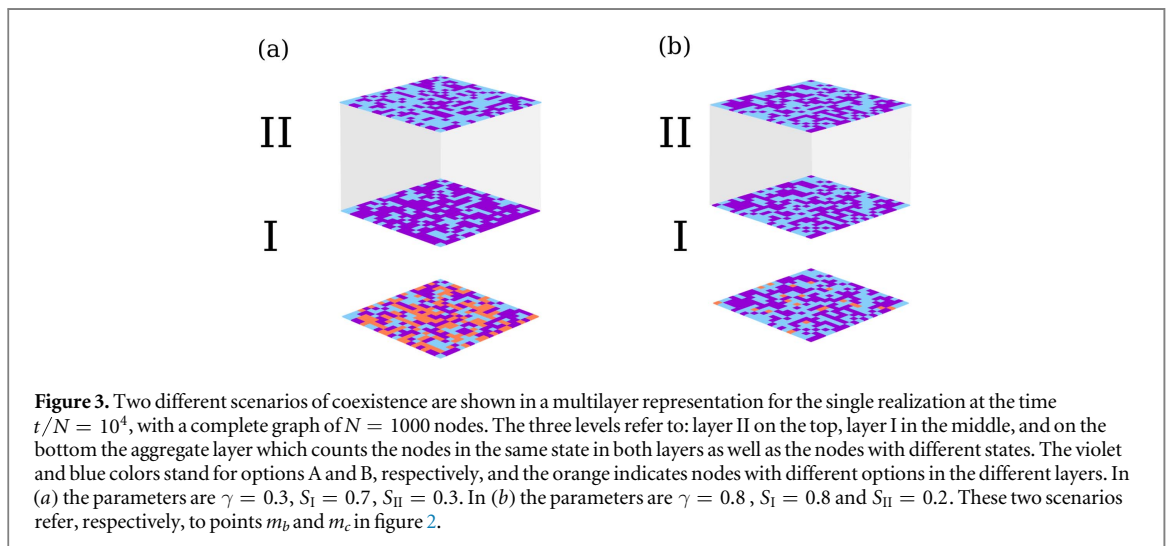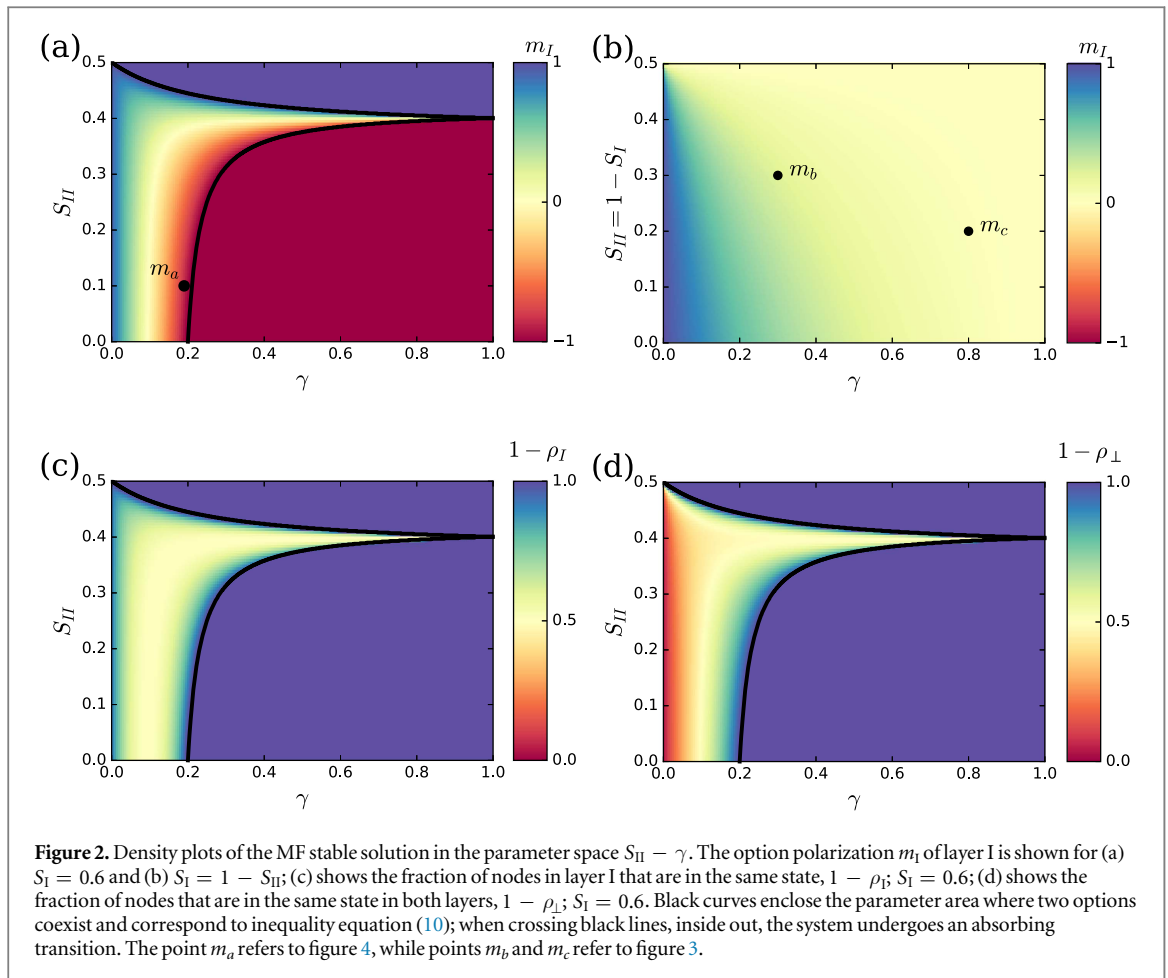2. One that stands for the non-consensus steady state where options A and B coexist and is given by,

$$\begin{aligned} m_I^* &= \frac{-2 + \sqrt{\frac{a}{b}}\sqrt{ab - 4}}{a}, \\ m_{II}^* &= \frac{+2 - \sqrt{\frac{b}{a}}\sqrt{ab - 4}}{b}, \end{aligned} \tag{9}$$

where $a = (1-\gamma)(2S_I - 1)/\gamma$ and $b = (1-\gamma)(2S_{II} - 1)/\gamma$. The stability of the fixed points is analyzed by imposing $\partial_{m_\alpha} V = 0$ and by studying the eigenvalues of the corresponding Jacobian matrix. We find that in the range of parameters defined by the relation:
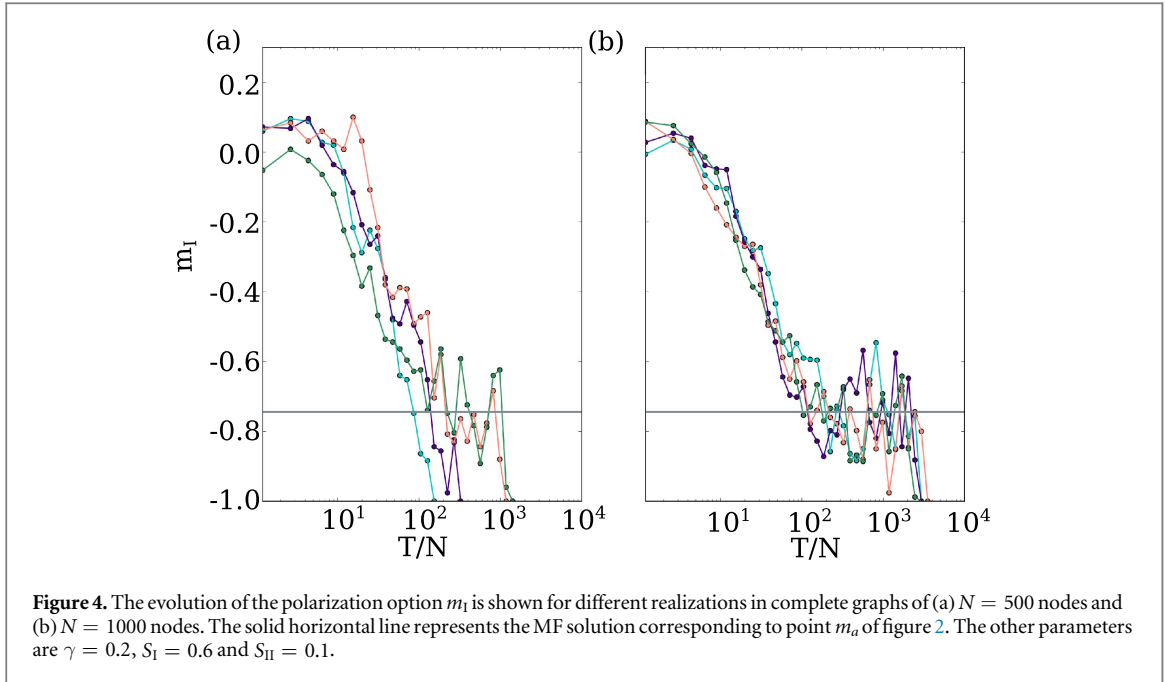
$$\frac{a}{a-1} \leqslant b \leqslant -\frac{a}{a+1}, \tag{10}$$

the steady state of coexistence, given by equation (9), is linearly stable while the state of full consensus is unstable. Out of this region, instead, the state of coexistence vanishes and the states of full consensus become stable; for $b > -\frac{a}{a+1}$ the system consents to option A, while for $b < \frac{a}{a-1}$ it consents to B. By substituting $b = -\frac{a}{a+1}$ in equation (9) we have $m_I = m_{II} = 1$, while by substituting $b = \frac{a}{a-1}$, $m_I = m_{II} = -1$. This means that out of the region expressed by equation (10), the two solutions of full consensus and coexistence coincide. The coexistence solution varies continuously from -1 to 1 generating a second order absorbing phase transition. The steady states of full consensus are absorbing, frozen states and the switch probabilities vanish. The steady state of coexistence, instead, is an active dynamical state (see [32]), where individuals continue switching and the system visits a set of configurations which are macroscopically equivalent in terms of ordering. Therefore, by varying parameters according to equation (10) we find an absorbing transition in which the system goes from an active state to a frozen configuration state.

The complementary of the density of active links, $1 - \rho_\alpha$, gives what is called the *coherent domain* [33], namely the density of links between nodes in the same state. Figure 2 shows the landscape of steady states of system equation (9) in the parameter space $\gamma - S^{II}$ for a fixed S^I. For $\gamma = 0$ the two layers do not communicate and the multiplex is reduced to two independent AS systems (see equation (1)). Each layer reaches a steady state of consensus; however, the states are complementary, i.e. one layer consents to option A while the other consents to option B. For $\gamma = 1$, both a and b are equal to zero and each solution of the form $m_I = m_{II}$ is a potential stable solution. The two layers communicate with the stronger possible coupling but the individuals are not affected by their neighbors (see equation (1)). A randomly chosen node replicates its state from the other layer, resulting in a frozen steady state where every node has the same state across the layers, while none of the layers reaches consensus. For other values of γ, the previously found condition equation (10) determines three different dynamical regimes displayed in figure 2 (for $0 \leqslant \gamma < 1$). Figure 2(a) shows the polarization option m_I of layer I. For $b > -\frac{a}{a+1}$, the system consents to option A (the violet area) while option B dominates for $b < \frac{a}{a-1}$ (the red area). For the other parameter values the two options coexist (the area enclosed by black curves). The resulting

Figure 2. Density plots of the MF stable solution in the parameter space $S_{II} - \gamma$. The option polarization m_I of layer I is shown for (a) $S_I = 0.6$ and (b) $S_I = 1 - S_{II}$; (c) shows the fraction of nodes in layer I that are in the same state, $1 - \rho_I$; $S_I = 0.6$; (d) shows the fraction of nodes that are in the same state in both layers, $1 - \rho_\perp$; $S_I = 0.6$. Black curves enclose the parameter area where two options coexist and correspond to inequality equation (10); when crossing black lines, inside out, the system undergoes an absorbing transition. The point m_a refers to figure 4, while points m_b and m_c refer to figure 3.

Figure 3. Two different scenarios of coexistence are shown in a multilayer representation for the single realization at the time $t/N = 10^4$, with a complete graph of $N = 1000$ nodes. The three levels refer to: layer II on the top, layer I in the middle, and on the bottom the aggregate layer which counts the nodes in the same state in both layers as well as the nodes with different states. The violet and blue colors stand for options A and B, respectively, and the orange indicates nodes with different options in the different layers. In (a) the parameters are $\gamma = 0.3$, $S_I = 0.7$, $S_{II} = 0.3$. In (b) the parameters are $\gamma = 0.8$, $S_I = 0.8$ and $S_{II} = 0.2$. These two scenarios refer, respectively, to points m_b and m_c in figure 2.

density of the connected nodes lying in the same states is presented in figure 2(c), while the density of coherent nodes between the layers, namely the nodes in the same state in both layers, is depicted in figure 2(d). We verify the results obtained from our MF approximation by constructing multiplex networks of different sizes composed of complete networks in their layers. In the coexistence regime, the options are distributed between the nodes in two different ways presented in figure 3. In figure 3(a), the parameter values allow the existence of both nodes in different states in the different layers and nodes in the same state across layers. The densities ρ_α and $\rho_\perp$ of the active links are different from zero. In figure 3(b), γ is strong enough to drive the system in a steady state, where the nodes have the same state in both layers. However, small fluctuations from this steady state are

Figure 4. The evolution of the polarization option m_I is shown for different realizations in complete graphs of (a) $N = 500$ nodes and (b) $N = 1000$ nodes. The solid horizontal line represents the MF solution corresponding to point m_a of figure 2. The other parameters are $\gamma = 0.2$, $S_I = 0.6$ and $S_{II} = 0.1$.

observed. The intra-layer densities $\rho_{I,II}$ of the active links are different from zero, while the inter-layer density $\rho_\perp$ fluctuates with a very small amplitude around zero.

4. Finite size effects in multiplex networks with complete layers

As mentioned above, the coexistence state is an active one, namely the probabilities of switching the state do not vanish and the system keeps fluctuating around the fixed point. In finite size networks, however, these fluctuations can drive the system to an absorbing state of full consensus. This is a finite size effect and has been observed in our stochastic simulations. In our settings, the two layers have opposite prestiges; therefore for $\gamma = 0$ the polarization option m_I would go to 1 while m_{II} would go to -1.
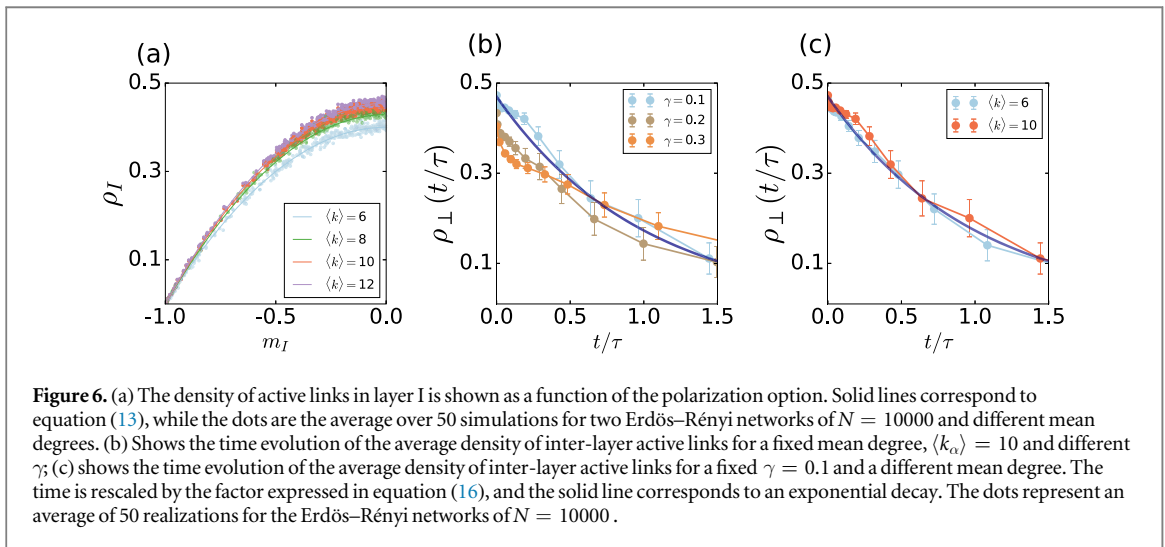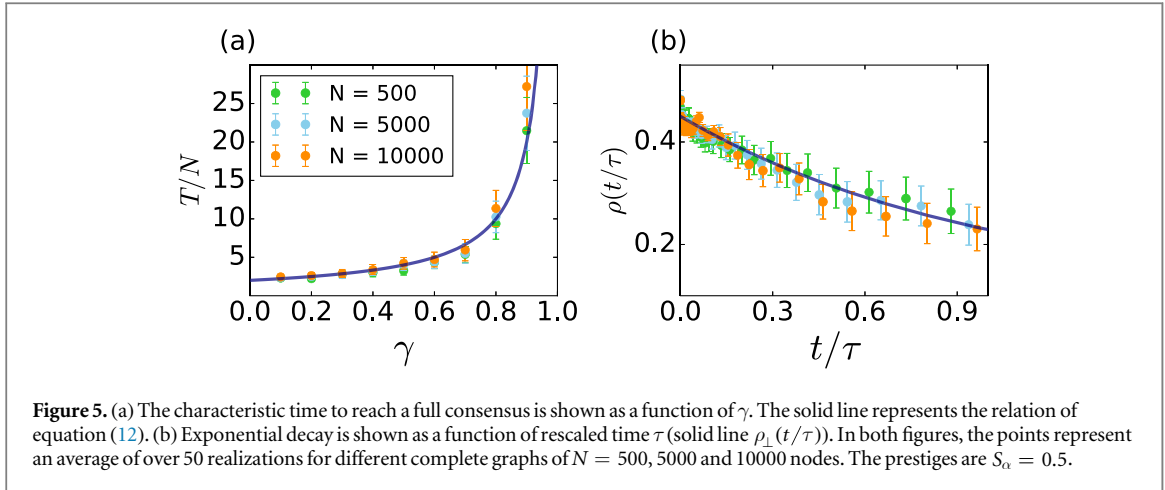
Figure 4 shows the evolution of m_I for different realizations in the case of complete networks of (a) $N = 500$ nodes and (b) $N = 1000$ nodes. In this particular setting of parameters ($\gamma = 0.2$, $S_I = 0.6$ and $S_{II} = 0.1$) the MF stable solution (the solid horizontal line) denotes a coexistence steady state but the fluctuations due to the finite size effect bring it to a full consensus in option B, with both $m_\alpha = -1$. The time the system remains around the MF solution depends on the size of the system and on the values of the parameters. A different case is the unbiased model where both the prestiges are equal, $S_\alpha = 1/2$. The potential reduces to

$$V_{\frac{1}{2}} = \frac{1}{2}\gamma(m_I - m_{II})^2 \tag{11}$$

and each solution of the form $m_I = m_{II}$ is a solution. In this particular setting we can study the effects purely induced by the multiplex structure, because we can avoid the effect generated by the competition between the two options in the two layers. From the related theory for single-layer networks [31] we know that in this case the system will reach an absorbing state with a characteristic time that scales with N. In the multiplex networks considered here we find by fitting (see figure 5) a factor arising from the inter-layer interaction, $c(\gamma) = \frac{1}{1-\gamma}$, for which the characteristic time to reach consensus takes the form

$$\tau = 2N\frac{1}{1-\gamma} = 2Nc(\gamma). \tag{12}$$

This relation is consistent with the studies presented in [31], where the scaling factor is the inverse of the prefactor of the active links in the diffusion coefficient. The factor $2N$ results from the total number of nodes in the whole two-layer system. From the time evolution expressed in [31], we can approximate $\rho_\perp(t) \approx e^{-t/\tau}$. Figure 5(a) shows the characteristic time equation (12) for a different size and different γ, using complete networks. Figure 5(b) shows the evolution of the density $\rho_\perp$ of the active inter-layer links. We can thus conclude that in the case of equal prestige, the multiplex effect translates into an extension $c(\gamma)$ in the lifetime of the coexistence option state.

Figure 5. (a) The characteristic time to reach a full consensus is shown as a function of γ. The solid line represents the relation of equation (12). (b) Exponential decay is shown as a function of rescaled time τ (solid line $\rho_\perp(t/\tau)$). In both figures, the points represent an average of over 50 realizations for different complete graphs of $N = 500$, 5000 and 10000 nodes. The prestiges are $S_\alpha = 0.5$.

Figure 6. (a) The density of active links in layer I is shown as a function of the polarization option. Solid lines correspond to equation (13), while the dots are the average over 50 simulations for two Erdös–Rényi networks of $N = 10000$ and different mean degrees. (b) Shows the time evolution of the average density of inter-layer active links for a fixed mean degree, $\langle k_\alpha \rangle = 10$ and different γ; (c) shows the time evolution of the average density of inter-layer active links for a fixed $\gamma = 0.1$ and a different mean degree. The time is rescaled by the factor expressed in equation (16), and the solid line corresponds to an exponential decay. The dots represent an average of 50 realizations for the Erdös–Rényi networks of $N = 10000$.

5. Erdös–Rényi networks

Here we extend the ansatz of [31] by considering Erdös–Rényi networks. In [31], it was found for the density of active links that the relation $\rho = \frac{1}{2}\psi(1 - m^2)$ is valid for a complex network of mean degree $\langle k_\alpha \rangle$, where $\psi = \frac{\langle k_\alpha \rangle - 2}{\langle k_\alpha \rangle - 1}$. We test this assumption for multiplex networks consisting of different Erdös–Rényi layers of various size and mean degree, discovering that it is also valid in our case (see figure 6).

Then, the density of intra-layer active links reads

$$\rho_\alpha = \frac{1}{2}\psi_\alpha(1 - m_\alpha^2). \tag{13}$$

The inter-layer density, instead, does not depend on the topology of the network. In order to extend the Fokker–Planck equation (7), for the case of two Erdös–Rényi networks we consider that if a node with k_α changes its state at a time step, the polarization option changes by $\pm\delta_{k,\alpha}$, with $\delta_{k,\alpha} = \frac{2k_\alpha}{\langle k_\alpha \rangle N}$. Since each node has an inter-layer degree equal to one, the inter-layer change remains $\frac{2}{N}$. Substituting relation 13 in the transition probabilities expressed in equation (A.1) and the right expression for $\pm\delta_{k,\alpha}$, we obtain for the Fokker–Plank equation $\partial_t Q_\alpha = -\partial_{m_\alpha}[\partial_{m_\alpha} V Q_\alpha] + \frac{1}{2N}\partial^2_{m_\alpha}[D_\alpha Q_\alpha]$, the following terms

$$\partial_{m_\alpha} V = (1 - \gamma)(2S - 1)\rho_\alpha + \gamma(m_{\bar\alpha} - m_\alpha),$$

$$D_\alpha = \frac{\langle k_\alpha^2 \rangle}{\langle k_\alpha \rangle^2}(1 - \gamma)\rho_\alpha + \gamma\rho_\perp. \tag{14}$$

Previous studies of the voter model (prestige equal to $1/2$) in complex networks [31], have revealed the relation between the characteristic time it takes to reach the full consensus and the topology of the network. Previously in [31], for an Erdös–Rényi network with a mean degree $\langle k \rangle$ a scaling factor was found of the form

$$T_{\text{ER}} = \frac{\langle k \rangle (\langle k \rangle - 1)}{(\langle k \rangle + 1)(\langle k \rangle - 2)} N. \tag{15}$$

By imposing $\gamma = 0$, the diffusion coefficient D_α of equation (14) reduces to a one layer case $D = \frac{\langle k^2 \rangle}{\langle k \rangle^2} \rho_\alpha = \frac{\langle k^2 \rangle}{\langle k \rangle^2} \psi(1 - \rho^2)$. Notice that the expression T_{ER} is the inverse of the prefactor of the density of the active links term. In our multiplex extension, by setting $S_a = \frac{1}{2}$ we check the same relation for the scaling factor by considering that the prefactor of the active links term ends up being a one layer term multiplied by $1 - \gamma$,
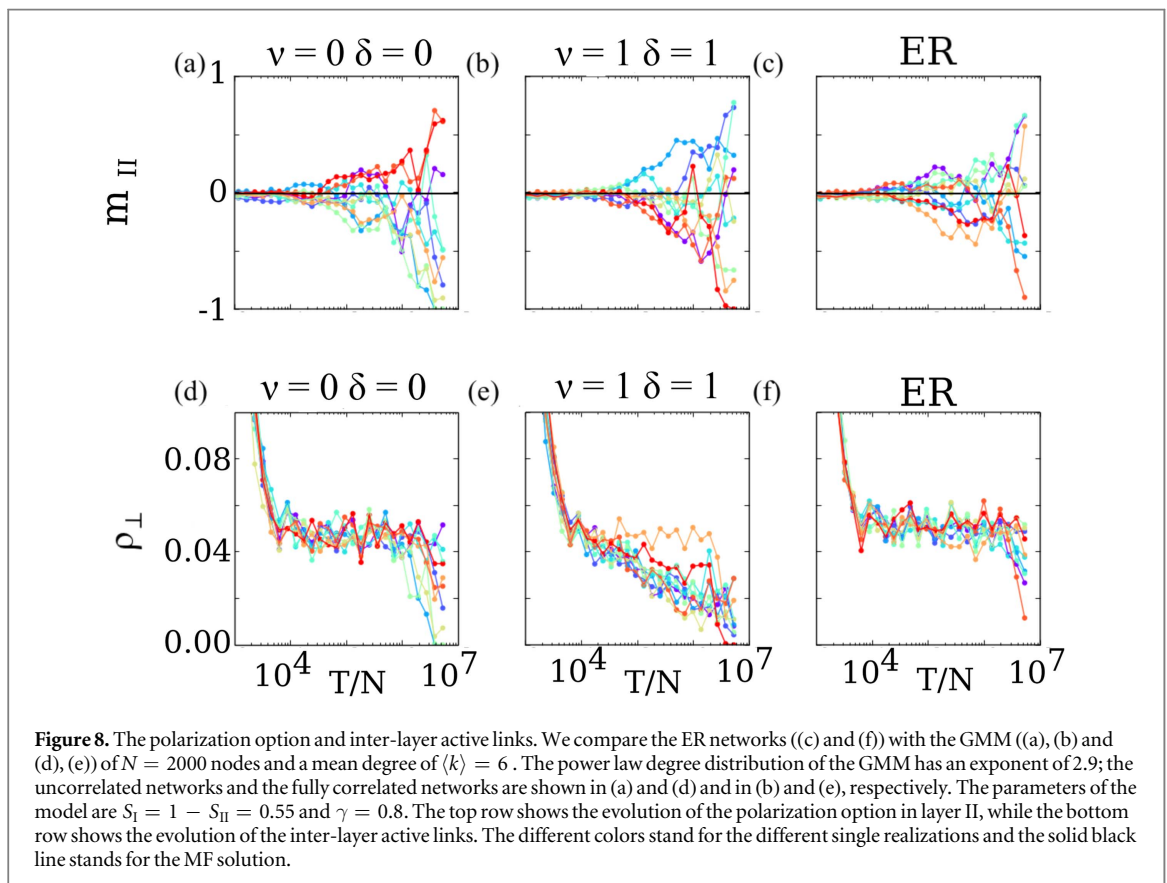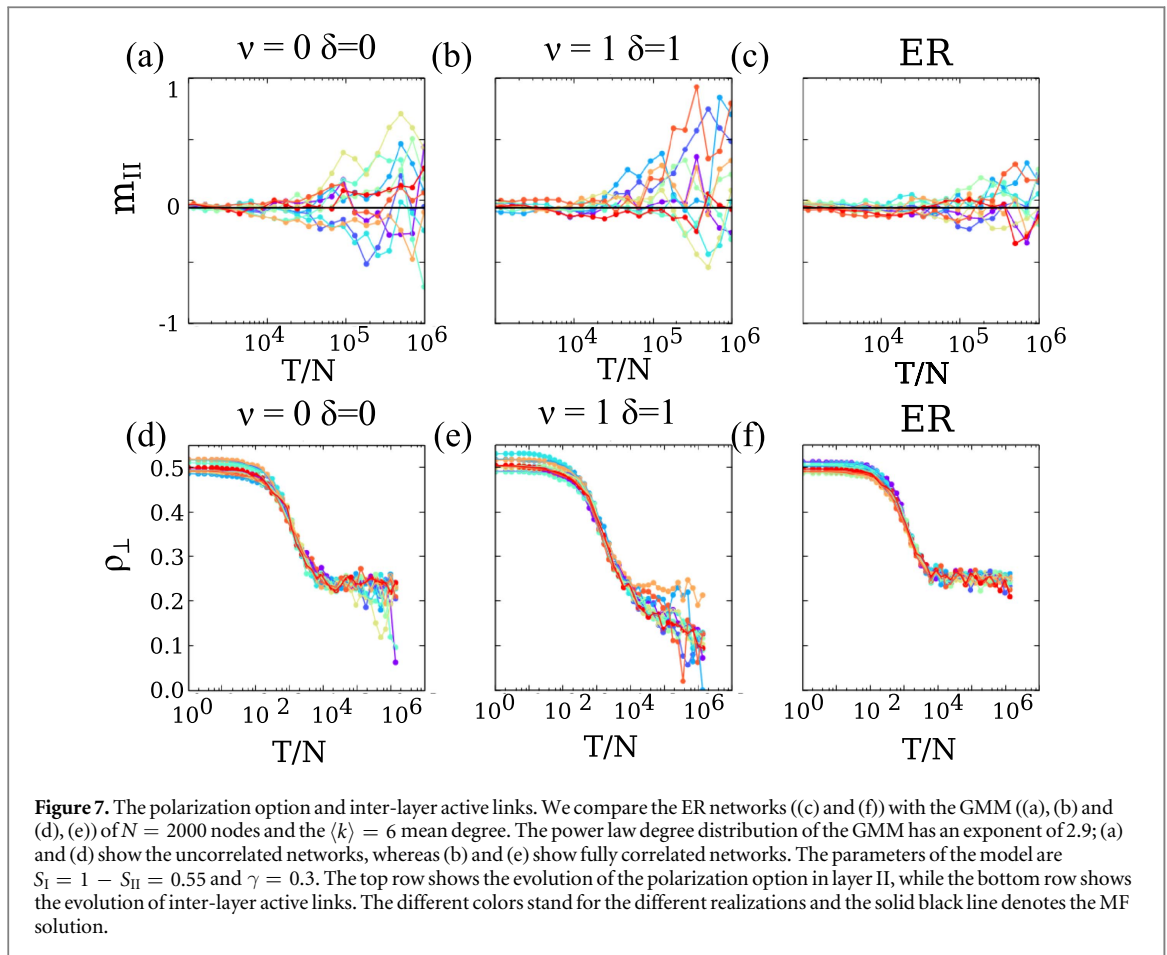
$$\tau = 2c(\gamma) T_{\text{ER}}. \tag{16}$$

As in the case of equation (12), a factor two accounts for the total number of nodes $2N$. In figures 6(a) and (b), we observe the time evolution of the average density $\rho_\perp$ of inter-layer active links for a fixed mean degree $\langle k_\alpha \rangle$ and different values of γ, showing the validity of the assumption expressed by equation (16).
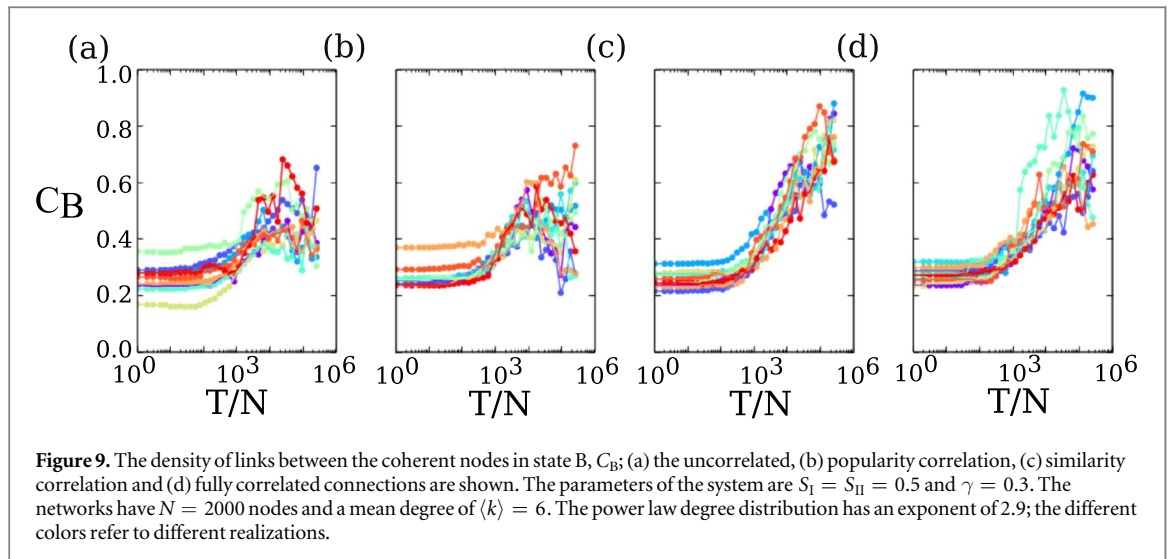
6. Impact of correlation

With a fully connected population we have shown how the coupling of two layers with two different preferred options can generate various kinds of coexistence options. Here we are interested in how the topology of two networks and the correlations between layers can influence the distribution of the states among the nodes. Previously, it was shown that the relation between the layers in a real multiplex can be characterized by geometric correlations in hidden metric spaces underlying each layer of the system [34–36]. There are two kinds of correlations: *popularity correlations*, which are correlations between the degrees the nodes have in the two layers, and *similarity correlations*, which control the probability of the links overlapping between layers. To understand the impact of correlations, we perform numerical simulation using the geometric multiplex model (GMM) developed in [34].

The GMM is based on the (single-layer) network construction procedure of the Newtonian $\mathbb{S}^1$ [37] and hyperbolic $\mathbb{H}^2$ [38] models. Here we present the treatment for the $\mathbb{H}^2$ version. To construct a network of N nodes, first it is requirement of the procedure for each node $i = 1, \ldots, N$ to be assigned its popularity r_i and similarity θ_i coordinates, and accordingly, to connect each pair of nodes i, j with the probability $p(x_{ij}) = 1/(1 + e^{\frac{1}{2T}(x_{ij} - R)})$, where x_{ij} is the hyperbolic distance between the nodes and $R \sim \ln N$. The connection probability $p(x_{ij})$ is the Fermi–Dirac distribution, where the temperature parameter T controls the level of clustering in the network [39]. The multiplex composed of these single-layer networks allows for radial and angular coordinate correlations across layers. The level of these correlations is regulated by the parameters $\delta \in [0, 1]$ and $\nu \in [0, 1]$, without affecting the single-layer topologies, where δ stands for the radial (also called popularity) correlation and ν denotes the angular (also called similarity) correlation. The popularity correlation relates to the probability of finding a node with the same degree in the different layers. The similarity correlation is related to the probability of the links overlapping between layers.

We compare the GMM with different correlation settings and with the ER networks. In all cases the multiplex networks are composed of layers of $N = 2000$ nodes with a mean degree of $\langle k \rangle = 6$. The most significant effect is observed in the distribution of the states between the nodes. The similarity correlation, which increases the probability of links overlapping between layers, promotes inter-layer groups of nodes in the same state and connected in both layers, namely coherent islands. If the whole system has a favorite state ($S_{\text{I}} \neq 1 - S_{\text{II}}$), finite size effects bring the system to an absorbing state of full consensus, in which the coherent islands of that state increase at the expense of the other. To appreciate the correlation effects, we consider the case of symmetric prestige. Figure 7 shows the evolution of the polarization option m_{II} (top row) and the inter-layer active links $\rho_\perp$ (bottom row) for $S_{\text{I}} = 1 - S_{\text{II}} = 0.55$ and $\gamma = 0.3$. Figures 7(a) and (d) refer to a GMM with uncorrelated layers, figures 7(b) and (e) refer to a GMM with fully correlated layers, while figures 7(c) and (f) refer to the ER networks. The behavior of $\rho_\perp$ is significantly different for the correlated and uncorrelated case. For the ER and uncorrelated GMM, $\rho_\perp$ fluctuates around the MF solution. Instead, in the strongly correlated system, the size of the coherent islands grows, generating a slower decay of $\rho_\perp$. The top row of figure 7 shows that none of the three systems has reached an absorbing state, for which the basic difference lies in the distribution of the states between nodes. We can conclude that the strongly correlated system is in a state of coexistence of different coherent islands. This feature becomes more evident for high values of the coupling, as shown in figure 8 where $\gamma = 0.8$. In this case, for some realizations, the system reaches full consensus in two different ways: in the uncorrelated case it is thanks to a single fluctuation from the finite size effects, while in the fully correlated case one of the coherent islands grows and incorporates the entire system. Another important measure reveals how the similarity correlation acts on the distribution of the states between nodes. In figure 9 we set $S_\alpha = 0.5$, for which neither the layers nor any of the system has a favored state (the coupling is $\gamma = 0.3$). In figure 9(a), the system is uncorrelated (i.e. $\delta = 0$ and $\nu = 0$), in figure 9(b) $\delta = 1$ and $\nu = 0$, in figure 9(c) $\delta = 0$ and $\nu = 1$ and in figure 9(d) $\delta = 1$ and $\nu = 1$. C_{B} defines the coherent island in option B, namely the

Figure 7. The polarization option and inter-layer active links. We compare the ER networks ((c) and (f)) with the GMM ((a), (b) and (d), (e)) of $N = 2000$ nodes and the $\langle k \rangle = 6$ mean degree. The power law degree distribution of the GMM has an exponent of 2.9; (a) and (d) show the uncorrelated networks, whereas (b) and (e) show fully correlated networks. The parameters of the model are $S_I = 1 - S_{II} = 0.55$ and $\gamma = 0.3$. The top row shows the evolution of the polarization option in layer II, while the bottom row shows the evolution of inter-layer active links. The different colors stand for the different realizations and the solid black line denotes the MF solution.

Figure 8. The polarization option and inter-layer active links. We compare the ER networks ((c) and (f)) with the GMM ((a), (b) and (d), (e)) of $N = 2000$ nodes and a mean degree of $\langle k \rangle = 6$. The power law degree distribution of the GMM has an exponent of 2.9; the uncorrelated networks and the fully correlated networks are shown in (a) and (d) and in (b) and (e), respectively. The parameters of the model are $S_I = 1 - S_{II} = 0.55$ and $\gamma = 0.8$. The top row shows the evolution of the polarization option in layer II, while the bottom row shows the evolution of the inter-layer active links. The different colors stand for the different single realizations and the solid black line stands for the MF solution.

Figure 9. The density of links between the coherent nodes in state B, C_{B}; (a) the uncorrelated, (b) popularity correlation, (c) similarity correlation and (d) fully correlated connections are shown. The parameters of the system are $S_{\mathrm{I}} = S_{\mathrm{II}} = 0.5$ and $\gamma = 0.3$. The networks have $N = 2000$ nodes and a mean degree of $\langle k \rangle = 6$. The power law degree distribution has an exponent of 2.9; the different colors refer to different realizations.

density of links overlaps the nodes in state B in both layers. We notice that C_{B} increases considerably when we set a similarity correlation ν equal to one. By comparing figure 9(a) with figures 9(b) and (c) we notice that the action of the popularity correlation alone does not produce significant effects, while the similarity correlation increases the coherent islands.

7. Conclusion

In this article we studied the consensus and coexistence of two opposing options in a discrete system organized in multiplex networks. For this purpose, we proposed a modification of the well-known AS model. Individuals correspond to the nodes of a multiplex and participate in different social networks in distinct layers. Social interaction within a given social context is denoted by intra-layer links, while inter-layer links represent the tendency to maintain the same option across different social networks. Although similar models have previously been studied in multiplex networks [4, 16, 17], the novelty of our study lies in the fact that individuals can have different options in different layers. This naturally reflects a common situation in which an individual can possess different opinions in different social contexts as a result of consensus with other individuals in one context but not in the other.

Our analysis shows that the latter property enriches the system dynamics and allows not only a consensus on a single state for both layers, but also for active dynamical states of coexistence for both options. This can be described by two layers having opposite preferred options, which generate potentials with the opposite minimum (there is no state that satisfies both layers). Each layer 'feels' the other to be an additive noise, so that even if individuals instantly consent in one layer, they preserve the chance of switching due to the influence of the other. In the MF approximation we found a coexistence phase: there is a wide range of parameters where the coexistence of the two options in each layer is in a stable steady state. An absorbing transition exists when going from this active phase of dynamical coexistence to the absorbing state of consensus. The transition lines are the ones indicated in figure 2, so that it can be induced by changing the coupling parameter between the layers. Beyond the mean field approximation we need to take into account finite size fluctuations. These fluctuations can drive the system from the active dynamical state of coexistence to an absorbing state of consensus. In particular, we considered the case of equally prestigious options, as in the voter model. For a single decoupled layer, the characteristic time it takes to reach an absorbing state is proportional to the size of the system [8]. In our case, indeed, because we have additive noise induced by the mutual influence between the layers, this characteristic time also depends on the coupling parameter γ. Therefore, in the presence of finite size fluctuations, the multiplex structure of our system can affect and lengthen the lifetime of the transient state of dynamical coexistence.

Mean field results are verified by numerical simulations in multiplex networks consisting of complete graphs, Erdös–Rényi networks and geometrical multiplex networks. For the Erdös–Rényi networks we find the same qualitative findings, but local effects modify the transition lines for the absorbing transition and lifetimes of active states depending on the distribution of degrees in the network. With geometrical multiplex networks we examined both the impact of network topology and the correlation between layers on the dynamics. We find that high correlations between layers promote the coexistence of different inter-layer islands of nodes in the same

state for small values of coupling, while high values of coupling facilitate the achievement of a full consensus state.

Acknowledgments

Appendix

We derive the master equation for the probability $Q(m_\alpha, t)$ where the system has the polarization option m_α at time t. If at a given time step δt a node changes its state, the polarization option changes by $2/N$. The probabilities of the possible changes in m_α are

$$W\left(m_\alpha \to m_\alpha + \frac{2}{N}\right) = \left[(1-\gamma)S_\alpha\rho_\alpha + \frac{\gamma}{4}(1-m_\alpha)(1+m_{\bar\alpha})\right],$$
$$W\left(m_\alpha \to m_\alpha - \frac{2}{N}\right) = \left[(1-\gamma)(1-S_\alpha)\rho_\alpha + \frac{\gamma}{4}(1+m_\alpha)(1-m_{\bar\alpha})\right],$$
$$W(m_\alpha \to m_\alpha) = 1 - (1-\gamma)\rho_\alpha - \gamma\rho_\perp. \tag{A.1}$$

Then, the probability of having the polarization option m_α at time t, $Q(m_\alpha, t + \delta t)$ reads

$$Q_\alpha = \sum_{k_\alpha} W\left(m_\alpha + \frac{2}{N} \to m_\alpha\right)Q\left(m_\alpha + \frac{2}{N}, t\right) + W\left(m_\alpha - \frac{2}{N} \to m_\alpha\right)Q\left(m_\alpha - \frac{2}{N}, t\right)$$
$$+ W(m_\alpha \to m_\alpha)Q(m_\alpha, t), \tag{A.2}$$

where Q_α stands for $Q(m_\alpha, t + \delta t)$.

Substituting the transition probability and considering that $\delta t = 1/2N$, we find the Fokker–Plank diffusion equation

$$\partial_t Q_\alpha = \partial_{m_\alpha}\left\{\left[\frac{1}{2}(1-\gamma)(1-2S_\alpha)(1-m_\alpha^2) + \frac{\gamma}{2}(m_\alpha - m_{\bar\alpha})\right]Q_\alpha\right\} + \frac{1}{N}\partial_{m_\alpha}^2\left\{\left[\frac{1}{2}(1-\gamma)(1-m_\alpha^2)\right.\right.$$
$$\left.\left. + \frac{\gamma}{2}(1-m_\alpha m_{\bar\alpha})\right]Q_\alpha\right\}. \tag{A.3}$$

We can rewrite the Fokker–Plank equation in the diffusive form

$$\partial_t Q_\alpha = -\partial_{m_\alpha}[\partial_{m_\alpha}VQ_\alpha] + \frac{1}{2N}\partial_{m_\alpha}^2[D_\alpha Q_\alpha], \tag{A.4}$$

where

$$\partial_{m_\alpha}V = (1-\gamma)(2S-1)\rho_\alpha + \gamma(m_{\bar\alpha} - m_\alpha) \tag{A.5}$$

and

$$D_\alpha = (1-\gamma)\rho_\alpha + \gamma\rho_\perp. \tag{A.6}$$

ORCID iDs

R Amato https://orcid.org/0000-0003-3817-8368
N E Kouvaris https://orcid.org/0000-0002-1975-2443
M San Miguel https://orcid.org/0000-0001-6237-425X
A Díaz-Guilera https://orcid.org/0000-0002-3114-0984

References

[1] Castellano C, Fortunato S and Loreto V 2009 Statistical physics of social dynamics *Rev. Mod. Phys.* **81** 591

[2] Patriarca M and Leppanen T 2004 Modeling language competition *Physica A* **338** 296–9
[3] Carro A, Toral R and San M M 2016 Coupled dynamics of node and link states in complex networks: a model for language competition *New J. Phys.* **18** 113056
[4] Halu A, Zhao K, Baronchelli A and Bianconi G 2013 Connect and win: the role of social networks in political elections *EPL* **102** 16002
[5] Clifford P and Sudbury A 1973 A model for spatial conflict *Biometrika* **60** 581–8
[6] Thomas M L and Richard A H 1975 Ergodic theorems for weakly interacting infinite systems and the voter model *Ann. Probab.* **3** 643–63
[7] Suchecki K, Eguíluz V M and San M M 2005 Voter model dynamics in complex networks: role of dimensionality, disorder, and degree distribution *Phys. Rev. E* **72** 036132
[8] Castellano C, Loreto V, Barrat A, Cecconi F and Parisi D 2005 Comparison of voter and Glauber ordering dynamics on networks *Phys. Rev. E* **71** 066107
[9] Abrams D M and Strogatz S H 2003 Modelling the dynamics of language death *Nature* **424** 342–51
[10] Stauffer D, Castelló X, Eguíluz V M and San M M 2007 Microscopic Abrams–Strogatz model of language competition *Physica A* **374** 835–42
[11] Withers C W J 1984 Gaelic in Scotland, 1698-1981: the geographical history of a language *Northern Scotland* **6** 204–6
[12] Charles W 1994 Review of a geography of the Welsh language (Aitchison, J and Carter, H) *Prog. Hum. Geogr.* **18** 551–2
[13] Vazquez F, Castelló X and San M M 2010 Agent based models of language competition: macroscopic descriptions and order-disorder transitions *J. Stat. Mech.* **2010** 4007
[14] Pinasco J P and Romanelli R 2006 Coexistence of languages is possible *Physica A* **361** 355–60
[15] Patriarca M, Castelló X, Uriarte J R, Eguíluz V M and San M M 2012 Modelling two-language competition dynamics *Adv. Complex Syst.* **15** 1250048
[16] Diakonova M, Nicosia V, Latora V and Miguel M S 2016 Irreducibility of multilayer network dynamics: the case of the voter model *New J. Phys.* **18** 023010
[17] Klimek P, Diakonova M, Eguíluz V M, San M M and Thurner S 2016 Dynamical origins of the community structure of an online multi-layer society *New J. Phys.* **18** 083045
[18] Gomez-Gardenes J, De Domenico M, Gutierrez G, Arenas A and Gomez S 2015 *Phil. Trans. R. Soc.* A **373** 2056
[19] De Domenico M, Solé-Ribalta A, Cozzo E, Kivelä M, Moreno Y, Porter M A, Gómez S and Arenas A 2013 Mathematical formulation of multilayer networks *Phys. Rev. X* **3** 041022
[20] Solé-Ribalta A, De Domenico M, Kouvaris N E, Díaz-Guilera A, Gómez S and Arenas A 2013 Spectral properties of the Laplacian of multiplex networks *Phys. Rev. E* **88** 032807
[21] Kivelä M, Arenas A, Barthelemy M, Gleeson J P, Moreno Y and Porter M A 2014 Multilayer networks *J. Complex Netw.* **2** 203–71
[22] Cardillo A, Gómez-Gardeñes J, Zanin M, Romance M, Papo D, del Pozo F and Boccaletti S 2013 Emergence of network features from multiplexity *Sci. Rep.* **3** 1344
[23] Morris R G and Barthelemy M 2012 Transport on coupled spatial networks *Phys. Rev. Lett.* **109** 128703
[24] Kurant M and Thiran P 2006 Layered complex networks *Phys. Rev. Lett.* **96** 138701
[25] Granell C, Gómez C and Arenas A 2013 Dynamical interplay between awareness and epidemic spreading in multiplex networks *Phys. Rev. Lett.* **111** 128701
[26] Vazquez F, Serrano M and San M M 2016 Rescue of endemic states in interconnected networks with adaptive coupling *Sci. Rep.* **6** 29342
[27] Kouvaris N E, Hata S and Diaz-Guilera A 2015 Pattern formation in multiplex networks *Sci. Rep.* **5** 10840
[28] Asllani M, Busiello D M, Carletti T, Fanelli D and Planchon G 2014 Turing patterns in multiplex networks *Phys. Rev. E* **90** 042814
[29] Battiston F, Nicosia V, Latora V and San M M 2017 Layered social influence promotes multiculturality in the Axelrod model *Sci. Rep.* **7** 1
[30] Kleineberg K K and Boguñá M 2015 Digital ecology: coexistence and domination among interacting networks *Sci. Rep.* **5** 10268
[31] Vazquez F and Eguíluz V M 2008 Analytical solution of the voter model on uncorrelated networks *New J. Phys.* **10** 063011
[32] Castelló X, Eguiluz V M, San M M, Loureiro-Porto L, Toivonen R, Saramäki J and Kaski K 2008 Modelling language competition: bilingualism and complex social networks *Proceedings of the 7th International Conference (EVOLANG7)* (Singapore: World Scientific) 59–66
[33] Toivonen R, Castelló X, Eguíluz V M, Saramäki J, Kaski K and San M M 2009 Broad lifetime distributions for ordering dynamics in complex networks *Phys. Rev. E* **79** 016109
[34] Kleineberg K K, Boguñá M, Serrano M A and Fragkiskos P 2016 Hidden geometric correlations in real multiplex networks *Nat. Phys* **12** 1076–81
[35] Boguñá M, Pastor-Satorras R and Vespignani A 2003 Absence of epidemic threshold in scale-free networks with degree correlations *Phys. Rev. Lett.* **90** 028701
[36] Kleineberg K K and Boguñá M 2015 Digital ecology: coexistence and domination among interacting networks *Sci. Rep.* **5** 10268
[37] Serrano M A, Krioukov D and Boguñá M 2008 Self-similarity of complex networks and hidden metric spaces *Phys. Rev. Lett.* **100** 078701
[38] Krioukov D, Papadopoulos F, Kitsak M, Vahdat A and Boguñá M 2010 Hyperbolic geometry of complex networks *Phys. Rev. E* **82** 036106
[39] Dorogovtsev S N 2010 *Lectures on Complex Networks* (Oxford: Oxford University Press)